

# Shadow Region Imaging Algorithm with Aperture Synthesis of Multiple Scattered Waves for UWB Radars

Shouhei KIDERA\*, Takuya SAKAMOTO and Toru SATO  
Graduate School of Informatics, Kyoto University, Japan  
Email:kidera@aso.cce.i.kyoto-u.ac.jp

## 1 Introduction

Ultra-wide band (UWB) pulse radar is promising as a near field sensing technique with high range resolution. As such, it is applicable to non-contact measurement of precision devices with specular surfaces, or to security systems that can identify a human body in invisible situations. For these applications, the SAR (Synthetic Aperture Radar) algorithm is still promising, as it creates a stable and accurate target image even in the near field [1]. However, in the case of complex or multiple targets, this algorithm suffers from increased shadow regions or false images caused by multiple scattered waves. In most case, a multiple scattered wave propagates a different path from that of a single scattered wave. This means that the multiple scattered echo has independent information on target surfaces, and thus has the potential to improve the image quality of the conventional methods, which use only single scattered waves. Although the time reversal algorithms with multiple scattered waves have been proposed, when focusing on target detection or positioning in cluttered situations [2-4], these require a target modeling or a priori information of the surrounding environment such as the walls. To relax these conditions, this paper proposes a direct imaging algorithm based on aperture synthesis of multiple scattered echoes. As a novelty of this paper, the proposed method is applicable to arbitrary target shapes, and directly enlarges the visible range on the target surface. Results obtained from numerical simulation verify the effectiveness of the proposed method.

## 2 System Model

Fig. 1 illustrates the system model, which assumes that the target has high conductivity such as a metal, and an arbitrary shape with a clear boundary. The propagation speed of the radio wave  $c$  is assumed to be known constant. An omnidirectional antenna is scanned along the  $x$ -axis. We use a mono-cycle pulse as the transmitting current. The real space in which the target and antenna are located is expressed by the parameters  $\mathbf{r} = (x, z)$ , which are normalized by  $\lambda$ , the central wavelength of the pulse.  $s(X, Z)$  is defined as the output of the Wiener filter at the antenna location  $(x, z) = (X, 0)$ , where  $Z = ct/(2\lambda)$  is expressed by the time  $t$ .

## 3 Conventional Algorithm

The SAR algorithm can create a stable and accurate target image even in the near field. The distribution image  $I_1(\mathbf{r})$  obtained with this algorithm is calculated as

$$I_1(\mathbf{r}) = \int_{X \in \Gamma} s\left(X, \sqrt{(x-X)^2 + z^2}\right) dX, \quad (1)$$

where  $\Gamma$  is the scanning range of the antenna. The target boundary can be extracted from its focused image  $I_1(\mathbf{r})$ . Below, we present two examples of this method, using a complex and multiple targets, respectively. The left and right hand side of Fig. 2 illustrates the outputs of the Wiener filter from the complex target and multiple targets, respectively, where each signal is received at 101 locations for  $-2.5 \leq X \leq 2.5$ . The conductivity of each target is set to  $1.0 \times 10^6$  S/m. The left and right hand sides of Fig. 3 show the images obtained using the conventional method for each target case. Each image is normalized by the maximum value of  $I_1(\mathbf{r})$ . The left hand side of Fig. 3 shows that the obtained image  $I_1(\mathbf{r})$  expresses only sharp edges on triangle boundaries, and not the greater part of the target surface that falls into a shadow region. The right hand side of Fig. 3 also shows difficulty in imaging the side of the rectangular target. This is because each antenna does not receive a direct reflection echo from the side of the target boundary with a large inclination. This is an inherent problem in imaging algorithms that only use single scattered echoes for target reconstruction.

#### 4 Proposed Algorithm

To overcome the problem described in the previous section, this paper proposes a shadow region imaging algorithm based on aperture synthesis of double scattered echoes. Except diffraction wave, a double scattered wave propagates a different path from that of a single scattered one, and this wave often includes significant information of two reflection points on the target boundaries. Then, a suitable use of these echoes is promising as shadow region imaging. This imaging method calculates the image using double scattered waves from the initial image  $I_1(\mathbf{r})$  as

$$I_2(\mathbf{r}) = - \int_{\mathbf{r}' \in R} \int_{X \in \Gamma} I_1(\mathbf{r}') s(X, d(\mathbf{r}, \mathbf{r}', X)) dX dx' dz', \quad (2)$$

where  $\mathbf{r}' = (x', z')$  is defined,  $R$  is the region of the real space, and  $d(\mathbf{r}, \mathbf{r}', X) = \sqrt{(x - X)^2 + z^2} + \sqrt{(x' - X)^2 + z'^2} + \sqrt{(x - x')^2 + (z - z')^2}$  holds. The minus sign in Eq. (2) creates a positive image focused by double scattered waves, that have an inverse phase relationship compared to single scattered ones. Eq.(2) expresses the aperture synthesis of the received signals by only considering a double scattered path. Here, we assume that only the positive images of  $I_1(\mathbf{r})$  and  $I_2(\mathbf{r})$  are necessary for the target boundary extraction. Then, the proposed method determines the final image  $I(\mathbf{r})$  as,

$$I(\mathbf{r}) = I_1(\mathbf{r})H(I_1(\mathbf{r})) + I_2(\mathbf{r})H(I_2(\mathbf{r})) \quad (3)$$

where  $H(x)$  is defined as

$$H(x) = \begin{cases} 1 & (x \geq 0) , \\ 0 & (x < 0) . \end{cases} \quad (4)$$

The proposed method uses only the initial image  $I_1(\mathbf{r})$  and directly emphasizes the target regions, through which double scattered waves pass.

## 5 Performance Evaluation in Numerical Simulation

This section refers the two examples of the proposed method. The left hand side of Fig. 4 shows the image  $I(\mathbf{r})$  for the complex target, using the same data as in the left hand side of Fig. 2. This figure confirms that the side of the target can be reconstructed using the proposed method, which produces a significant image to determine the triangular boundary. Furthermore, the right hand side of Fig. 4 shows the image  $I(\mathbf{r})$  for multiple objects using the same data as in the right hand side of Fig. 2. This figure shows that the side region of the rectangular target can be identified, and that the visible ranges of the circle and rectangular boundaries are substantially enlarged. This is because the double scattered waves are effectively focused on the target side by Eq. (2), and the region around the either of double scattered points is visible in the initial image  $I_1(\mathbf{r})$ . Moreover, it is noteworthy that this method does not require a target modeling or a priori information of the surroundings, and yet it is a significant improvement from the conventional algorithms [2-4]. We also confirm that the image obtained by the proposed method remains accurate in a noisy situation, where the S/N of the double scattered signal is higher than 20 dB. However, false images appear behind the targets in each example, and these should be suppressed in future work. In addition, this method requires the triple integration of the received signals in Eq. (2), and this requires around 30 minutes for the calculation with a Xeon 2.8 GHz processor. Thus, an acceleration in the imaging speed is also required to the extended method to 3-dimensional problems.

## 6 Conclusion

This paper proposed the direct shadow region imaging algorithm based on aperture synthesis for double scattered waves. Because the conventional SAR algorithm uses only single scattered waves, the greater part of a complex target or multiple targets falls into a shadow region. To overcome this problem, we extended the SAR algorithm to use double scattered waves. The results from a numerical simulation verify that this method makes the shadow region visible, and enlarges the imaging range quite substantially without a priori information of target models or the surroundings. Although the proposed method requires a great deal of calculation, it has the potential to expand the application range of near field radar in cluttered situations.

## References

- [1] D. L. Mensa, G. Heidbreder and G. Wade, *IEEE Trans. Nuclear Science.*, vol. 27, no. 2, pp. 989–998, Apr, 1980.
- [2] S. K. Lehmann and A. J. Devaney, *Acoust. Soc. Am.*, 113 (5), May, 2003.
- [3] J. M. F. Moura, and Y. Jin, *IEEE Trans. on Signal Process.*, vol. 55, no. 1, pp. 187–201, Jan, 2007.
- [4] T. Kitamura, T. Sakamoto and T. Sato, *IEICE General Conference*, C-1-9, Mar, 2008 (in Japanese).

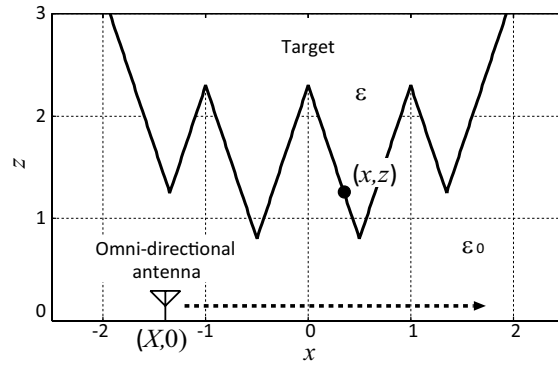


Figure 1: System model.

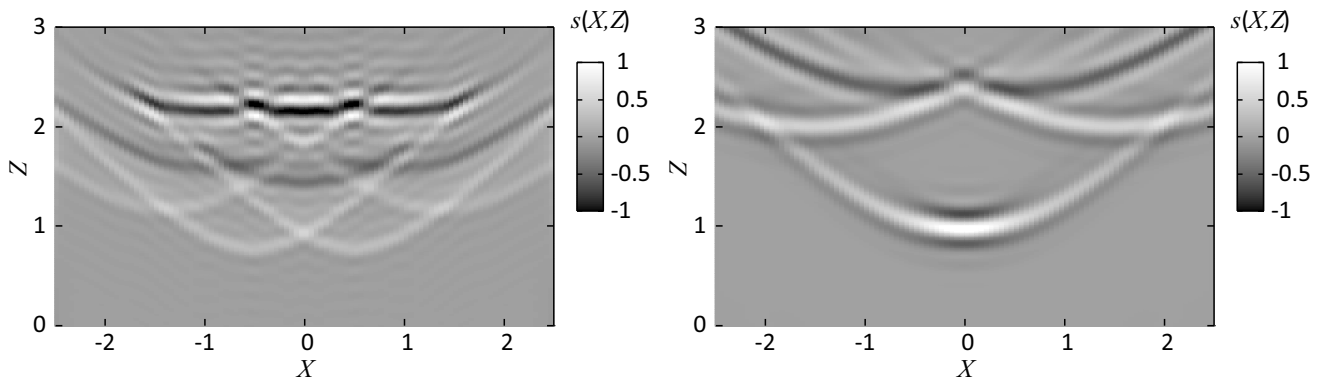


Figure 2: Outputs of Wiener filter from complex target (left) and multiple targets (right).

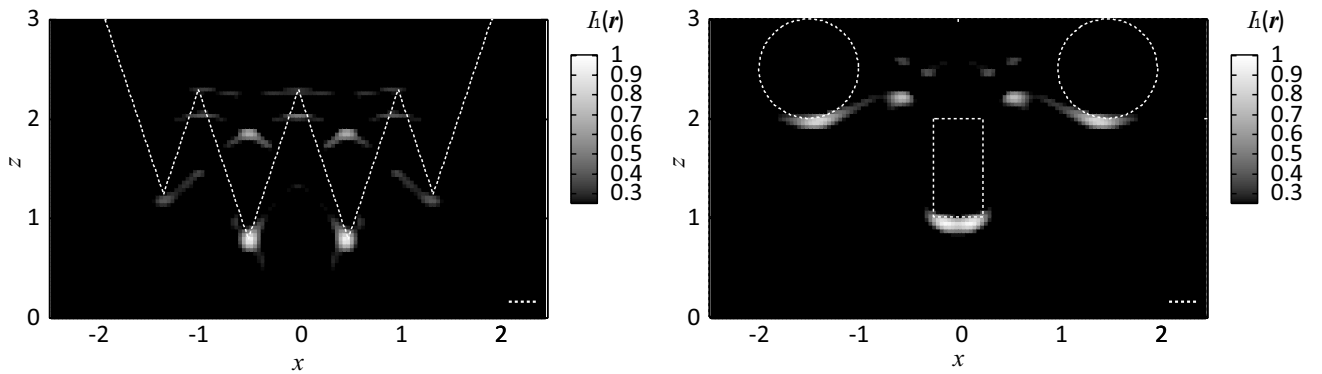


Figure 3: Estimated images with the conventional method for complex target (left) and multiple targets (right).

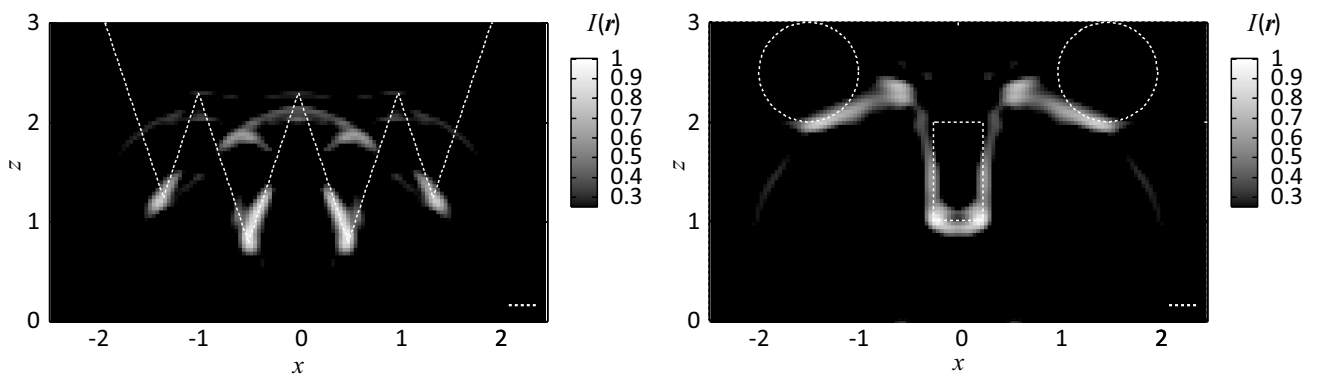


Figure 4: Estimated images with the proposed method for complex target (left) and multiple targets (right).